

The Top Window for dark matter

Kingman Cheung^{1,2,3}, Kentarou Mawatari^{4,5},

Eibun Senaha³, Po-Yan Tseng², and Tzu-Chiang Yuan⁶

¹*Division of Quantum Phases & Devices,*

School of Physics, Konkuk university, Seoul 143-701, Korea

²*Department of Physics, National Tsing Hua University, Hsinchu 300, Taiwan*

³*Physics Division, National Center for Theoretical Sciences, Hsinchu 300, Taiwan*

⁴*Institut für Theoretische Physik, Universität Heidelberg,*

Philosophenweg 16, D-69120 Heidelberg, Germany

⁵*Theoretische Natuurkunde and IIHE/ELEM,*

Vrije Universiteit Brussel, and International Solway Institutes,

Pleinlaan 2, B-1050 Brussels, Belgium ^a

⁶*Institute of Physics, Academia Sinica, Nankang, Taipei 11529, Taiwan*

(Dated: November 4, 2018)

Abstract

We investigate a scenario that the top quark is the only window to the dark matter particle. We use the effective Lagrangian approach to write down the interaction between the top quark and the dark matter particle. Requiring the dark matter satisfying the relic density we obtain the size of the effective interaction. We show that the scenario can be made consistent with the direct and indirect detection experiments by adjusting the size of the effective coupling. Finally, we calculate the production cross section for $t\bar{t} + \chi\bar{\chi}$ at the Large Hadron Collider (LHC), which will give rise to an interesting signature of a top-pair plus large missing energy.

^a Address since October 2010

I. INTRODUCTION

The presence of cold dark matter (CDM) in our Universe is now well established by a number of observational experiments, especially the very precise measurement of the cosmic microwave background radiation in the Wilkinson Microwave Anisotropy Probe (WMAP) experiment [1]. The measured value of the CDM relic density is

$$\Omega_{\text{CDM}} h^2 = 0.1099 \pm 0.0062 ,$$

where h is the Hubble constant in units of 100 km/Mpc/s. Though the gravitation nature of the dark matter is established, we know almost nothing about the particle nature, except that it is, to a high extent, electrically neutral.

One of the most appealing and natural CDM particle candidates is *weakly-interacting massive particle* (WIMP). It is a coincidence that if the dark matter is produced thermally in the early Universe, the required annihilation cross section is right at the order of weak interaction. The relation between the relic density and the thermal annihilation cross section can be given by the following simple formula [2]

$$\Omega_{\chi} h^2 \simeq \frac{0.1 \text{ pb}}{\langle \sigma v \rangle} , \quad (1)$$

where $\langle \sigma v \rangle$ is the annihilation rate of the dark matter around the time of freeze-out. Given the measured $\Omega_{\text{CDM}} h^2$ the annihilation rate is about 1 pb or $10^{-26} \text{ cm}^3 \text{ s}^{-1}$. This is exactly the size of the cross sections that one expects from a weak interaction process and that would give a large to moderate production rate at the LHC. In general, production of dark matter at the LHC would give rise to a large missing energy. Thus, the anticipated signature in the final state is high- p_T jets or leptons plus a large missing energy. Note that there could be non-thermal sources for the dark matter, such as decay from exotic relics like moduli fields, cosmic strings, etc. In such cases, the annihilation rate in Eq. (1) can be larger than the value quoted above.

The most studied dark matter candidate is perhaps the neutralino of the supersymmetric models with R -parity conservation. In this work, we study a different scenario. The dark matter is in a hidden sector and the only standard model (SM) particle that it interacts with is the top quark. The top quark, having a mass so close to the electroweak symmetry breaking scale, makes itself so unique among the fermions. It is perhaps one of the best

windows to probe the electroweak symmetry breaking. The dark matter, if it is a WIMP, is also closely related to electroweak symmetry breaking. The logic is that since both the top quark and the WIMP are closely related to electroweak symmetry breaking, we argue that the top quark may be the only window to probe the dark matter. This is our motivation.¹ We use an effective Lagrangian approach to parameterize the interactions between the top quark and the dark matter particle, without specifying the detailed communication between the top quark and the hidden sector. One simple example would be a hidden-sector gauge boson that can couple to the top quark. If it is heavy enough we can shrink the propagator to a 4-fermion vertex. One form of the 4-fermion interaction is $(\bar{t}\gamma_\mu t)(\bar{\chi}\gamma^\mu\chi)$ for a vector-type interaction or $(\bar{t}\gamma_\mu\gamma^5 t)(\bar{\chi}\gamma^\mu\gamma^5\chi)$ for an axial-vector-type interaction. We can estimate the size of the new interaction based on the fact that it is the only interaction that can thermalize the dark matter particle in the early Universe. The most interesting implication of the scenario is the collider signature. The final state consists of a top-quark pair and a pair of dark matter particles, giving rise to a top-quark pair plus a large missing energy. On the other hand, we anticipate that the spin-independent and spin-dependent cross sections in direct detection would be consistent with the current limit. This is easy to understand because the top content inside the nucleon is so small that it hardly contributes to the DM-nucleon scattering. We will explicitly show that. In addition, the annihilation of the dark matter in the Galactic Halo would give rise to positrons and antiprotons that can be observed by antimatter search experiments, e.g., PAMELA and AMSII. We use the present data on positron and antiproton spectra from PAMELA to constrain the size of the effective interactions.

The organization of the paper is as follows. In the next section, we describe the interaction between the top quark and the dark matter particle, and estimate the size of the interaction based on the relic density. In Sec. III, we calculate the spin-independent and spin-dependent cross sections for direct detection. In Sec. IV, we calculate the positron and antiproton spectra due to the DM annihilation in Galactic halo. In Sec. V, we discuss the collider signature. Finally, we conclude in Sec. VI.

There are a few recent works [4–6] that assumed some form of effective interactions between the dark matter and light quarks and studied the corresponding collider phenomenology. Fan *et al.* [7] also wrote down the effective nonrelativistic interactions between the

¹ A possibility of realizing such a scenario can be found in Ref. [3]

dark matter and nuclei.

II. EFFECTIVE INTERACTIONS AND RELIC DENSITY

Our simple model consists of the SM and a hidden sector, in which there is a pair of Dirac/Majorana fermions and a gauge boson. For some reasons this gauge boson couples this hidden fermion only to the top quark on the SM side. If the mass of this gauge boson is heavy enough, we can integrate it out. More generally, below the heavy mass scale Λ the interaction between the top quark and the dark matter particle, denoted by χ , is given by

$$\mathcal{L} = \frac{g_\chi^2}{\Lambda^2} (\bar{\chi}\Gamma\chi) (\bar{t}\Gamma t) , \quad (2)$$

where $\Gamma = \gamma^\mu$ for a vector gauge boson, $\Gamma = \gamma^\mu\gamma^5$ for an axial-vector gauge boson, $\Gamma = 1$ (γ^5) for a scalar (pseudoscalar) boson interaction, and $\Gamma = \sigma^{\mu\nu}$ (γ^5) with $\sigma^{\mu\nu} \equiv i(\gamma^\mu\gamma^\nu - \gamma^\nu\gamma^\mu)/2$ for a tensor (axial-tensor) interaction, and g_χ is an effective coupling constant. For Majorana fermions the $\Gamma = \gamma^\mu$ or $\sigma^{\mu\nu}$ type interaction is identically zero, and so for vector or tensor type interaction the fermion χ in Eq.(2) must be Dirac. Explicitly, we assume the dark matter candidate to be Dirac, but the results are also applicable to Majorana dark matter. With this interaction we can calculate the thermal averaged cross sections and thus the relic density, the direct and indirect detection rates, and also the production cross section of $pp \rightarrow t\bar{t} + \chi\bar{\chi}$ at the LHC.

We start with a vector gauge boson type interaction: $\Gamma = \gamma^\mu$. The differential cross section for $\chi(p_1) \bar{\chi}(p_2) \rightarrow t(k_1) \bar{t}(k_2)$, with the 4-momenta listed in the parentheses, is

$$\frac{d\sigma}{dz} = \frac{g_\chi^4}{\Lambda^4} \frac{N_C}{16\pi s} \frac{\beta_t}{\beta_\chi} [u_m^2 + t_m^2 + 2s(m_\chi^2 + m_t^2)] \quad (3)$$

where $N_C = 3$ for the top quark color, $\beta_{t,\chi} = (1 - 4m_{t,\chi}^2/s)^{1/2}$, $t_m = t - m_\chi^2 - m_t^2 = -s(1 - \beta_t\beta_\chi z)/2$, $u_m = u - m_\chi^2 - m_t^2 = -s(1 + \beta_t\beta_\chi z)/2$, $s = (p_1 + p_2)^2$ is the square of the center-of-mass energy, $t = (p_1 - k_1)^2$, $u = (p_1 - k_2)^2$, and $z \equiv \cos \Theta$ with Θ the scattering angle. The quantity σv , where $v \approx 2\beta_\chi$ in the non-relativistic limit, can be obtained by integrating over the variable z in Eq. (3). Instead of solving the Boltzmann equation, we can naively estimate the size of the interaction by the following equation

$$\Omega_\chi h^2 \simeq \frac{0.1 \text{ pb}}{\langle \sigma v \rangle} . \quad (4)$$

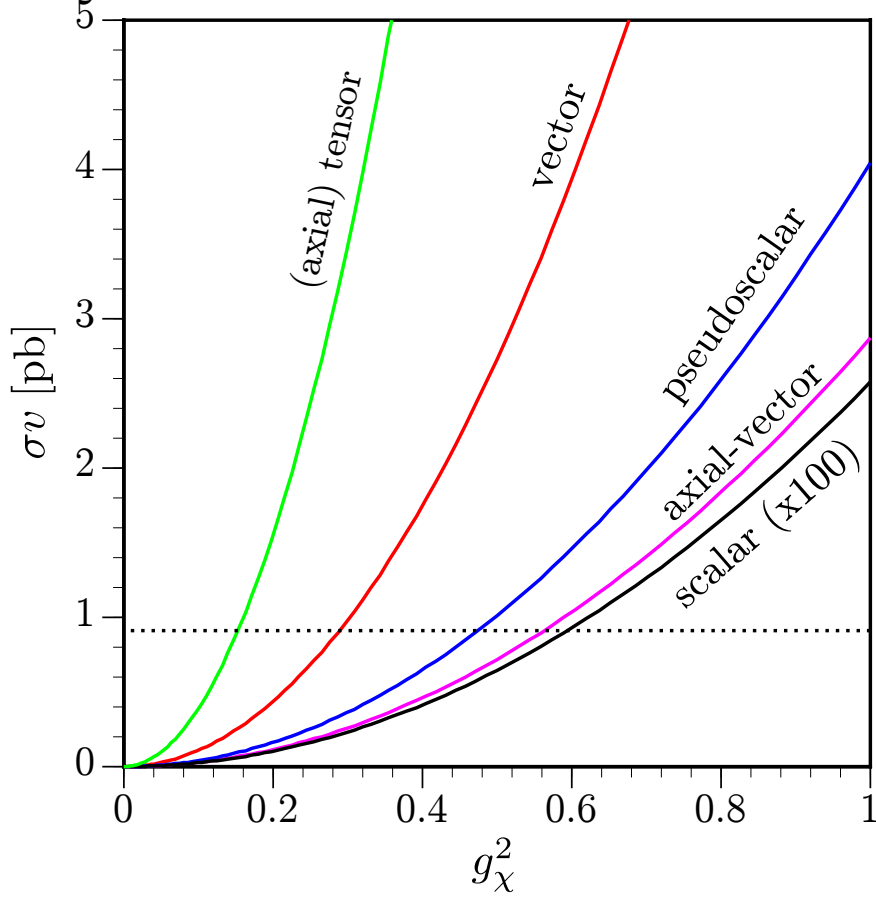


FIG. 1. The calculated σv versus g_χ^2 for the effective interaction $\frac{g_\chi^2}{\Lambda^2} (\bar{\chi}\Gamma\chi) (\bar{t}\Gamma t)$ of various Dirac structures Γ with $\Lambda = 1$ TeV, $m_\chi = 200$ GeV, and $v \approx 0.3$.

With the most recent WMAP result on dark matter density $\Omega_{\text{CDM}} h^2 = 0.1099 \pm 0.0062$ we obtain the size of σv

$$\langle \sigma v \rangle \simeq 0.91 \text{ pb} . \quad (5)$$

We show in Fig. 1 σv versus the coefficient g_χ^2 for a dark matter mass of 200 GeV. The result shown is for $v \approx 0.3$ to approximate the velocity of the dark matter particle at around the freeze-out time. We can repeat the calculation with $\Gamma = \sigma^{\mu\nu}(\gamma^5)$, $\gamma^\mu\gamma^5$, γ^5 , 1 for tensor

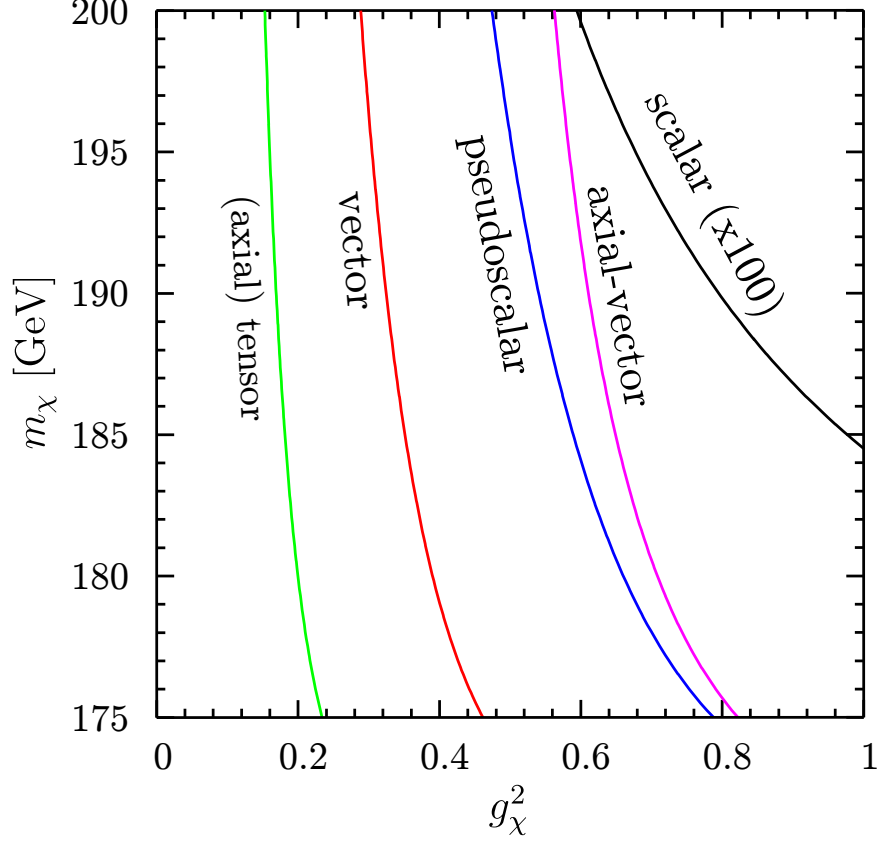


FIG. 2. Contours of $\sigma v = 0.91$ pb in the plane of (g_χ^2, m_χ) for vector, axial-vector, pseudoscalar, scalar, tensor and axial-tensor interactions. Λ is set at 1 TeV.

(axial-tensor), axial-vector, pseudoscalar, and scalar type interactions. The results are

$$\frac{d\sigma}{dz} = \frac{g_\chi^4 N_C}{\Lambda^4 4\pi s} \frac{\beta_t}{\beta_\chi} [2(t_m^2 + u_m^2) + 2s(m_t^2 + m_\chi^2) + 8m_t^2 m_\chi^2 - s^2] \quad (6)$$

$$\frac{d\sigma}{dz} = \frac{g_\chi^4 N_C}{\Lambda^4 16\pi s} \frac{\beta_t}{\beta_\chi} [t_m^2 + u_m^2 - 2s(m_t^2 + m_\chi^2) + 16m_t^2 m_\chi^2] \quad (7)$$

$$\frac{d\sigma}{dz} = \frac{g_\chi^4 N_C}{\Lambda^4 32\pi} s \frac{\beta_t}{\beta_\chi} \quad (8)$$

$$\frac{d\sigma}{dz} = \frac{g_\chi^4 N_C}{\Lambda^4 32\pi} s \beta_\chi \beta_t^3 \quad (9)$$

for $\Gamma = \sigma^{\mu\nu}(\gamma^5)$, $\gamma^\mu\gamma^5$, γ^5 , 1, respectively. We note that the axial-tensor case has the expression as in the tensor one given by Eq.(6). The results are shown in Fig. 1 as well. We can see that the tensor-type interaction gives the largest cross section, followed by vector, pseudoscalar, and axial-vector. These four types of interactions require g_χ^2 falling into the range of 0.2 – 0.6 which is about the size of weak-scale interaction. On the other hand,

the scalar-type interaction always gives a very small annihilation cross section for a similar range of g_χ^2 , which is in danger of over-closing the Universe.

In Fig. 2, we show the contour of the cross section for the various types of interactions as a function of g_χ^2 and m_χ as allowed by the WMAP result.

III. DIRECT DETECTION

Recently, the CDMSII finalized their search in Ref. [8]. When they opened the black box in their blind analysis, they found two candidate events, which are consistent with background fluctuation at a probability level of about 23%. Nevertheless, the signal is not conclusive. The CDMS then improves upon the upper limit on the spin-independent (SI) cross section $\sigma_{\chi N}^{\text{SI}}$ to 3.8×10^{-44} cm² for $m_\chi \approx 70$ GeV. The XENON100 Collaboration [9] also recently announced their newest result. Although XENON100 has the best sensitivity in the lower mass range, the CDMSII limit is currently still the best in the world for dark matter mass larger than about 100 GeV. We will adopt a limit of order $4 - 10 \times 10^{-44}$ cm² for dark matter mass of 200 – 500 GeV. In the following, we will check if the spin-independent cross section generated by the 4-fermion interactions is consistent with the new limit.

Spin-independent cross sections can arise from the scalar-type and vector-type interactions between the DM and quarks. If the effective interactions between the dark matter particle and the quarks are given by

$$\mathcal{L} = \sum_{q=u,d,s,c,b,t} \{ \alpha_q^S \bar{\chi} \chi \bar{q} q + \alpha_q^V \bar{\chi} \gamma^\mu \chi \bar{q} \gamma_\mu q \} , \quad (10)$$

then the spin-independent cross section between χ and each of the nucleon (taking the average between proton and neutron) is given by

$$\sigma_{\chi N}^{\text{SI}} = \frac{4\mu_{\chi N}^2}{\pi} \left(|G_s^N|^2 + \frac{|b_N|^2}{256} \right) , \quad (11)$$

where $\mu_{\chi N} = m_\chi m_N / (m_\chi + m_N)$ is the reduced mass between the dark matter particle and the nucleon N , and

$$G_s^N = \sum_{q=u,d,s,c,b,t} \langle N | \bar{q} q | N \rangle \alpha_q^S , \quad (12)$$

where $\langle N | \bar{q} q | N \rangle$ denotes the various nucleon matrix elements. The expression for b_N of a *whole nucleus* (A, Z) is $b_N \equiv \alpha_u^V (A + Z) + \alpha_d^V (2A - Z)$, we take the average between proton

and neutron (assume the number of protons is about the same as that of neutrons in the nuclei) and thus obtain the expression for a single nucleon

$$b_N = \frac{3}{2} (\alpha_u^V + \alpha_d^V) . \quad (13)$$

Nevertheless, the contributions to b_N come from valence quarks only. Therefore, in our scenario the only contribution to the SI cross section comes from the top quark, thus only α_t^S is nonzero in the expression of G_s^N , which is then given by

$$G_s^N = \langle N | \bar{t}t | N \rangle \left(\frac{g_\chi^2}{\Lambda^2} \right) , \quad (14)$$

where $\langle N | \bar{t}t | N \rangle = f_{Tt}^N (m_N/m_t)$.² The default value of the parameters f_{Tt}^N used, e.g. in DarkSUSY [10], is

$$f_{Tt}^p = 0.0595 , \quad f_{Tt}^n = 0.0592 .$$

Taking the average between proton and neutron the value of G_s^N is

$$G_s^N \simeq \frac{f_{Tt}^N m_N}{m_t} \left(\frac{g_\chi^2}{\Lambda^2} \right) . \quad (15)$$

For $m_\chi \sim O(100)$ GeV, $\mu_{\chi N} \approx m_N$. The spin-independent cross section is

$$\sigma_{\chi N}^{\text{SI}} \approx \frac{4\mu_{\chi N}^2}{\pi} \left(\frac{f_{Tt}^N m_N}{m_t} \right)^2 \left(\frac{g_\chi^2}{\Lambda^2} \right)^2 . \quad (16)$$

We show in Fig. 3 the spin-independent cross section versus g_χ^2 . Note that the axial-vector interactions contributes to spin-dependent cross sections. Since the constraint from spin-dependent cross sections is a few orders of magnitude weaker than that from spin-independent cross sections, we simply focus the spin-independent one to obtain the meaningful range of g_χ^2 and Λ . We found that the limit on spin-independent cross section of the order of 10^{-44} cm² allows g_χ^2 as large as 30 for $\Lambda = 1$ TeV. Note that for a strongly coupled theory, one can have $g^2 = (4\pi)^2$. Such a large g_χ^2 is allowed by spin-independent cross section constraint as well as by the WMAP relic density constraint.³ However, one must be cautious that for such a large effective coupling constant, perturbative calculation becomes less reliable.

We next turn to the indirect detection of the dark matter, which then gives the strongest constraint on the present scenario.

² Equivalently, the top content inside the nucleon can be replaced by the gluon content with f_{Tt}^N replaced by $\frac{2}{27} f_{Tg}^N$ [2]. Numerically, they are very close to each other.

³ When the annihilation cross section is larger than that required by thermal production, the resulting relic density from thermal production is just too low. However, there could be some other non-thermal sources, such as decay from heavier fields.

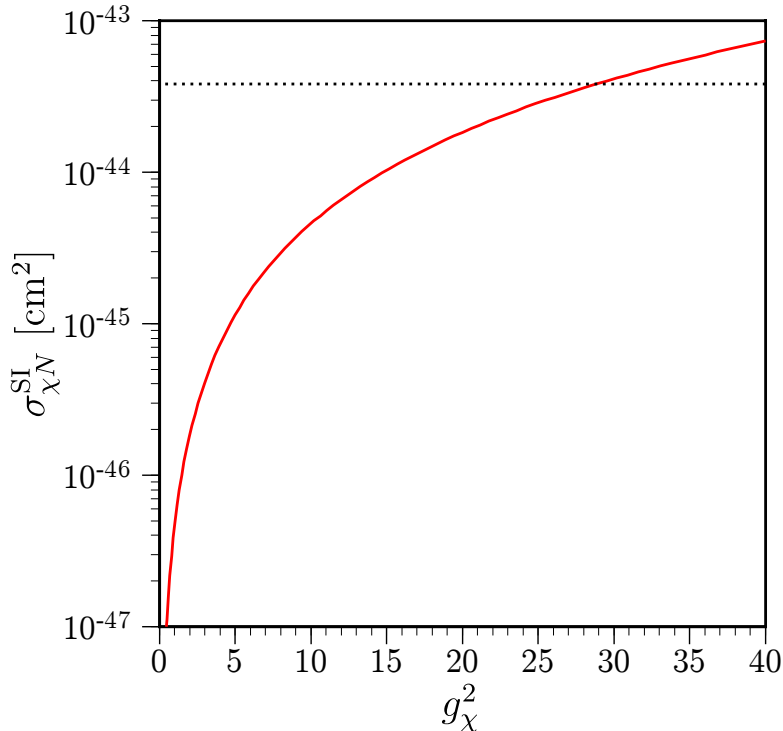


FIG. 3. Spin-independent cross sections for the vector type interaction versus g_χ^2 .

IV. INDIRECT DETECTION

Another important method to detect the dark matter is by measuring its annihilation products in Galactic halo. Current experiments can detect the positron, antiproton, gamma ray, and deuterium from dark matter annihilation. The Milky Way Halo may contain clumps of dark matter, from where the annihilation of dark matter particles may give rise to large enough signals, such as positron and antiproton, that can be identified by a number of antimatter search experiments. The most recent ones come from PAMELA [11, 12], which showed a spectacular rise in the positron spectrum but an expected spectrum for antiproton. It may be due to nearby pulsars or dark matter annihilation or decays. If it is really due to dark matter annihilation, the dark matter would have very strange properties, because it only gives positrons in the final products but not antiproton. Here we adopt a conservative approach. We use the observed antiproton and positron spectra as constraints on the annihilation products in $\chi\bar{\chi}$ annihilation.

We first consider the positron coming from the process

$$\chi\bar{\chi} \rightarrow t\bar{t} \rightarrow (bW^+)(\bar{b}W^-) \rightarrow (be^+\nu_e) + X \quad (17)$$

in which the most energetic e^+ comes from the W^+ decay. There are also positrons coming off in the subsequent decays of b, \bar{b}, τ^+ , or μ^+ , but these positrons are in general softer than those coming directly from the W^+ decay. For a first order estimate of the size of the coupling g_χ^2 in Eq. (2) we only include the positrons coming directly from the W^+ decay.

The expression for annihilation has already been given in Eq. (3), but now with a present time velocity $v \approx 10^{-3}$. The positron flux observed at the Earth is given by

$$\Phi_{e^+}(E) = \frac{v_{e^+}}{4\pi} f_{e^+}(E), \quad (18)$$

with v_{e^+} close to the velocity of light c . The function $f_{e^+}(E)$ satisfies the diffusion equation of

$$\frac{\partial f}{\partial t} - K(E)\nabla^2 f - \frac{\partial}{\partial E}(b(E)f) = Q, \quad (19)$$

where the diffusion coefficient is $K(E) = K_0(E/\text{GeV})^\delta$ and the energy loss coefficient is $b(E) = E^2/(\text{GeV} \times \tau_E)$ with $\tau_E = 10^{16}$ sec. The source term Q due to the annihilation is

$$Q_{\text{ann}} = \eta \left(\frac{\rho_{\text{CDM}}}{M_{\text{CDM}}} \right)^2 \sum \langle \sigma v \rangle_{e^+} \frac{dN_{e^+}}{dE_{e^+}}, \quad (20)$$

where $\eta = 1/2$ ($1/4$) for (non-)identical DM particle in the initial state. The summation is over all possible channels that can produce positrons in the final state, and dN_{e^+}/dE_{e^+} denotes the spectrum of the positron energy per annihilation in that particular channel. In our analysis, we employ the vector-type interaction for Dirac fermions and thus the source term is given by

$$Q_{\text{ann}} = \frac{1}{4} \left(\frac{\rho_{\text{CDM}}}{M_{\text{CDM}}} \right)^2 \langle \sigma v \rangle_{\chi\bar{\chi} \rightarrow t\bar{t}} \frac{dN_{e^+}}{dE_{e^+}}, \quad (21)$$

where the normalization of N_{e^+} is

$$\int \frac{dN_{e^+}}{dx} dx = B(t \rightarrow bW^+ \rightarrow be^+\nu_e). \quad (22)$$

We then put the source term into GALPROP [13] to solve the diffusion equation. In Fig. 4 we show the predicted energy spectrum for the positron fraction for various values of g_χ^2 . With a visual inspection the $g_\chi^2 \lesssim 8$ is allowed by the spectrum.

Next we turn to the antiproton fraction as it was also measured by PAMELA. Similarly, the antiproton flux can be obtained by solving the diffusion equation with the corresponding terms and the appropriate source term for the input antiproton spectrum:

$$Q_{\text{ann}} = \eta \left(\frac{\rho_{\text{CDM}}}{M_{\text{CDM}}} \right)^2 \sum \langle \sigma v \rangle_{\bar{p}} \frac{dN_{\bar{p}}}{dT_{\bar{p}}}, \quad (23)$$

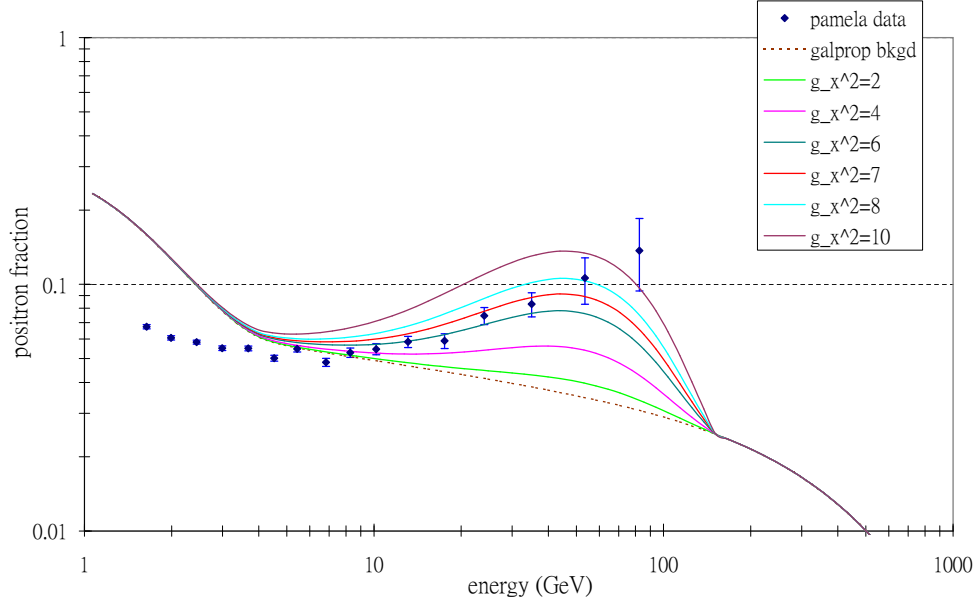


FIG. 4. Spectrum for the positron fraction predicted for the vector type interactions for various g_χ^2 . PAMELA data are shown.

where $\eta = 1/2$ ($1/4$) for (non-)identical initial state, and $T_{\bar{p}}$ is the kinetic energy of the antiproton which is conventionally used instead of the total energy. We again solve the diffusion equation using GALPROP [13].

In our case, the dominant contribution comes from

$$\chi\bar{\chi} \rightarrow t\bar{t} \rightarrow (bW^+)(\bar{b}W^-) \rightarrow (bq\bar{q}')(\bar{b}q\bar{q}') \rightarrow \bar{p} + X. \quad (24)$$

In the last step, all the $b\bar{b}, q, \bar{q}'$ have probabilities fragmenting into \bar{p} . We adopt a publicly available code [14] to calculate the fragmentation function $D_{q \rightarrow h}(z)$ for any quark q into hadrons h , e.g., p, \bar{p}, π . The fragmentation function is then convoluted with energy spectrum dN/dE of the light quark to obtain the energy spectrum of the antiproton $dN/dE_{\bar{p}}$. The source term $dN/dT_{\bar{p}}$ is then implemented into GALPROP to calculate the propagation from the halo to the Earth. We display the energy spectrum for the antiproton fraction in Fig. 5. It is easy to see that g_χ^2 is constrained to be

$$g_\chi^2 \lesssim 4 - 5. \quad (25)$$

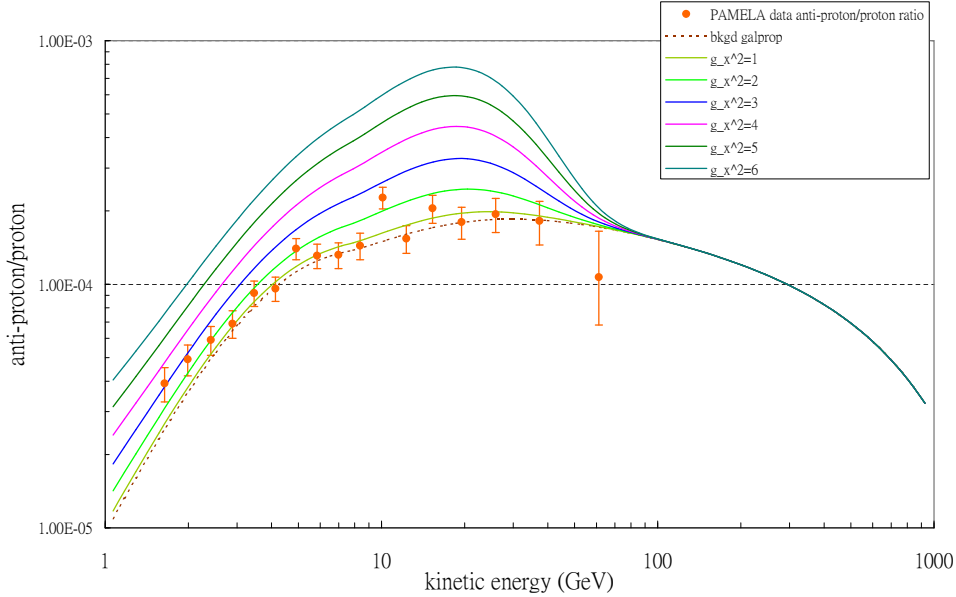


FIG. 5. Spectrum for the antiproton fraction predicted for the vector type interactions for various g_χ^2 . PAMELA data are shown.

We will use this allowed range to estimate what we would expect from the LHC.

V. COLLIDER SIGNATURE

Collider signatures are perhaps the most interesting part of the scenario – $t\bar{t}$ pair plus large missing energy. We first calculate using the effective 4-fermion interaction with $\Gamma = \gamma^\mu$ the production cross section for $pp \rightarrow t\bar{t} + \chi\bar{\chi}$. There are two contributing subprocesses for $t\bar{t}$ production at the LHC:

$$q\bar{q} \rightarrow t\bar{t}, \quad gg \rightarrow t\bar{t}, \quad (26)$$

on which we can attach one 4-fermion interaction vertex to each fermion leg including internal fermion line to further produce a $\chi\bar{\chi}$ pair. A typical Feynman diagram is shown in Fig. 6. We employ MADGRAPH [15] to calculate the signal and background cross sections.

The irreducible background is $t\bar{t} + Z \rightarrow t\bar{t}\nu\bar{\nu}$. Before applying any cuts we calculate

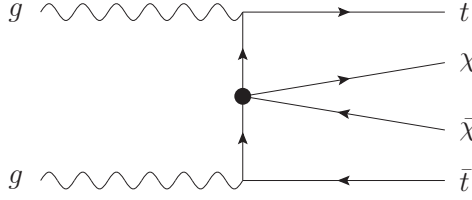


FIG. 6. A contributing Feynman diagram for the subprocess $gg \rightarrow t\bar{t} + \chi\bar{\chi}$. The other two diagrams can be obtained by attaching the black dot to the t and \bar{t} leg, respectively.

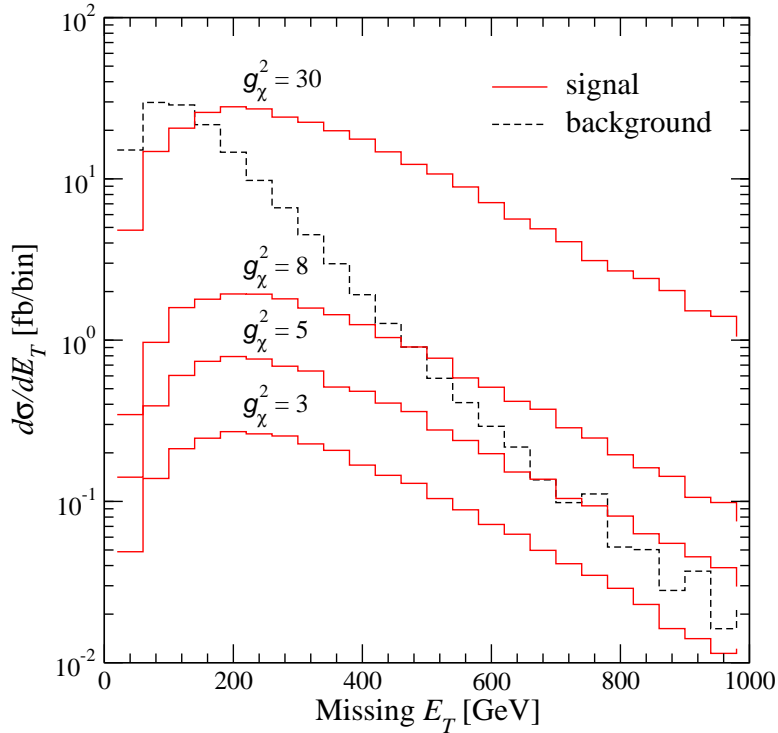


FIG. 7. Missing transverse energy E_T distributions for the signal $pp \rightarrow t\bar{t} + \chi\bar{\chi}$ and the background $pp \rightarrow t\bar{t}Z$ for $g_\chi^2 = 3 - 30$ with $m_\chi = 200$ GeV.

the signal cross section versus background cross section: 8.2 fb (for $g_\chi^2 = 5$) to 140 fb, in which we have chosen scale $Q = (2m_t + 2m_\chi)/2$ in the running coupling constant and the parton distribution functions for the signal, while $Q = (2m_t + m_Z)/2$ for the background. We first compare the missing E_T distribution between the dark matter signal and the $t\bar{t}Z$ background, shown in Fig. 7. It is clear that the signal has a harder missing E_T spectrum than the background. This plot suggests a cut as large as 400 GeV in the missing transverse energy can substantially reduce the background to a level similar to the signal. The cross sections in fb for the signal and the background using various cuts on the missing energy

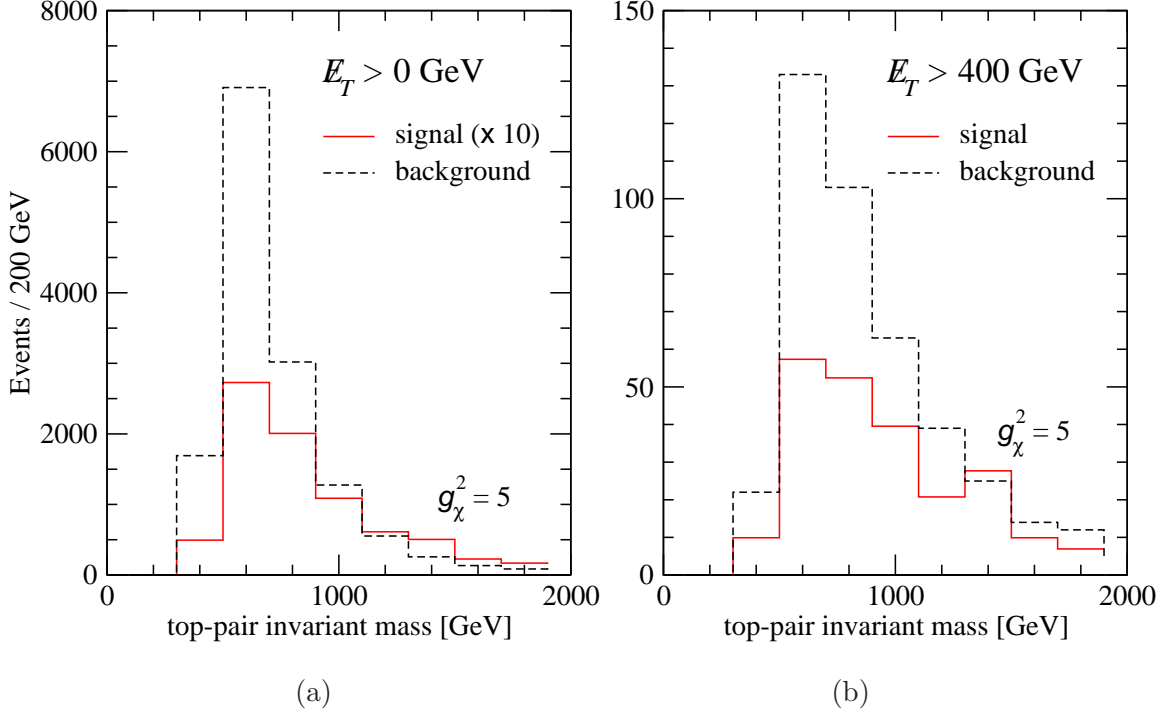


FIG. 8. Event numbers for the invariant mass $t\bar{t}$ distributions for the signal $pp \rightarrow t\bar{t} + \chi\bar{\chi}$ and the background $pp \rightarrow t\bar{t}Z$ (a) before and (b) after applying the missing transverse momentum cut of 400 GeV. The assumed luminosity is 100 fb^{-1} , which corresponds to 240 signal events and 420 background events after the cut.

are shown in Table I. The background can indeed be cut down to the level as the signal with a missing energy cut of 400 GeV. Note that the signal cross section scales as g_χ^4 . The significance of the signal S/\sqrt{B} for an integrated luminosity of 100 fb^{-1} stays around 11 with a cut of 300 – 500 GeV. Since the significance scales as $\sqrt{\mathcal{L}}$, with a reduced luminosity of 30 fb^{-1} the significance is still as large as 6.

We then compare the $t\bar{t}$ invariant mass distribution between the dark matter signal and the $t\bar{t}Z$ background before and after applying the missing E_T cuts, shown in Fig. 8. In Table II, we also show the signal cross sections and the significance for axial-vector, pseudoscalar, and scalar interactions ⁴ in decreasing order. Note that the cross section at the LHC for scalar interaction is not severely suppressed, in sharp contrast to the annihilation cross section calculated in Sec. II.

⁴ Note that the tensor interaction is not present in current version of MADGRAPH [15].

TABLE I. Cross sections in fb for the signal $pp \rightarrow t\bar{t} + \chi\bar{\chi}$ and the background $pp \rightarrow t\bar{t}Z \rightarrow t\bar{t} + \nu\bar{\nu}$ at the LHC. We used $g_\chi^2 = 5$ for illustration. The signal cross section scales as g_χ^4 . The significance S/\sqrt{B} is calculated with an integrated luminosity of 100 (30) fb^{-1} .

$E_T >$	$pp \rightarrow t\bar{t} + \chi\bar{\chi}$	$p \rightarrow t\bar{t}Z \rightarrow t\bar{t}\nu\bar{\nu}$	S/B	S/\sqrt{B} (100 (30) fb^{-1})
0 GeV	8.2	140.3	0.06	6.9 (3.8)
300 GeV	3.6	10.7	0.34	11.0 (6.0)
400 GeV	2.4	4.2	0.57	11.8 (6.4)
500 GeV	1.5	1.9	0.78	10.6 (5.9)

TABLE II. Cross sections in fb for the signal $pp \rightarrow t\bar{t} + \chi\bar{\chi}$ for vector, axial-vector, pseudoscalar, and scalar interactions at the LHC. We have imposed the $E_T > 400$ GeV cut. The S/B and S/\sqrt{B} are shown. The background is from Table I. The significance S/\sqrt{B} is calculated with an integrated luminosity of 100 (30) fb^{-1} .

	Signal cross section (fb)	S/B	S/\sqrt{B}
Vector	2.4	0.57	11.8 (6.4)
Axial-vector	1.9	0.45	9.3 (5.1)
Pseudoscalar	0.82	0.20	4.0 (2.2)
Scalar	0.55	0.13	2.7 (1.5)

VI. CONCLUSIONS

In this paper we have studied an interesting scenario where the dark matter couples exclusively to the top quark using an effective field theory approach, with the intuition that both the top quark and the dark matter may be closely related to electroweak symmetry breaking. We did not specify any particular connector linking the SM sector and the invisible dark matter sector, except that this connector sector was taken to be heavy, probably at the TeV scale. Integrating out the heavy connector sector may give rise to effective 4-fermion interactions of tensor, axial-tensor, vector, axial-vector, pseudoscalar, or scalar types between the dark matter and the top quark. We studied the constraints of these effective couplings from WMAP as well as from the direct and indirect detection of dark matter at

CDMSII and PAMELA, respectively.

If we require all the dark matter in the Universe comes from the thermal equilibrium, the coupling $g_\chi^2 \approx 0.3 - 0.6$. However, if we just require that the dark matter does not overclose the Universe the g_χ^2 can be much larger. Since only the top quark inside the nucleon contributes to direct detection cross section, the coupling g_χ^2 can be as large as 40. On the other hand, the strongest constraint comes from the positron and antiproton fraction spectra. The PAMELA antiproton spectrum constrains the coupling to be $g_\chi^2 \lesssim 4 - 5$.

This model can be tested at colliders with a very distinct signature, namely, $t\bar{t}$ plus missing energies. The top quark and antiquark would mostly have high p_T and boosted. The detection of such boosted top quarks has attracted some recent studies that it can be sufficiently distinguished from the background [16]. Our results suggested that this interesting scenario can be testable at the LHC.

ACKNOWLEDGMENTS

The work was supported in parts by the National Science Council of Taiwan under Grant Nos. 96-2628-M-007-002-MY3, 99-2112-M-007-005-MY3, and 98-2112-M-001-014-MY3, the NCTS, and the WCU program through the KOSEF funded by the MEST (R31-2008-000-10057-0).

-
- [1] J. Dunkley *et al.* [WMAP Collaboration], *Astrophys. J. Suppl.* **180**, 306 (2009).
 - [2] G. Bertone, D. Hooper, and J. Silk, *Phys. Rept.* **405**, 279 (2005) [arXiv:hep-ph/0404175].
 - [3] C. B. Jackson, G. Servant, G. Shaughnessy, T. M. P. Tait and M. Taoso, *JCAP* **1004**, 004 (2010) [arXiv:0912.0004 [hep-ph]]; M. Battaglia and G. Servant, arXiv:1005.4632 [hep-ex].
 - [4] Q. H. Cao, C. R. Chen, C. S. Li and H. Zhang, arXiv:0912.4511 [hep-ph];
 - [5] Y. Bai, P. J. Fox and R. Harnik, arXiv:1005.3797 [hep-ph];
 - [6] J. Goodman, M. Ibe, A. Rajaraman, W. Shepherd, T. M. P. Tait and H. B. P. Yu, arXiv:1005.1286 [hep-ph]; J. Goodman, M. Ibe, A. Rajaraman, W. Shepherd, T. M. P. Tait and H. B. P. Yu, arXiv:1008.1783 [hep-ph].
 - [7] J. Fan, M. Reece and L. T. Wang, arXiv:1008.1591 [hep-ph].

- [8] Z. Ahmed *et al.* [The CDMS-II Collaboration and CDMS-II Collaboration], arXiv:0912.3592 [astro-ph.CO].
- [9] E. Aprile *et al.* [XENON100 Collaboration], arXiv:1005.0380 [astro-ph.CO].
- [10] P. Gondolo, J. Edsjo, P. Ullio, L. Bergstrom, M. Schelke and E. A. Baltz, JCAP **0407**, 008 (2004) [arXiv:astro-ph/0406204].
- [11] O. Adriani *et al.* [PAMELA Collaboration], Nature **458**, 607 (2009).
- [12] O. Adriani *et al.*, Phys. Rev. Lett. **102**, 051101 (2009).
- [13] A. W. Strong, I. V. Moskalenko, T. A. Porter, G. Johannesson, E. Orlando and S. W. Digel, arXiv:0907.0559 [astro-ph.HE].
- [14] S. Albino, B. A. Kniehl and G. Kramer, Nucl. Phys. B **725**, 181 (2005).
- [15] F. Maltoni and T. Stelzer, JHEP **0302**, 027 (2003) [arXiv:hep-ph/0208156]; J. Alwall *et al.*, JHEP **0709**, 028 (2007) [arXiv:0706.2334 [hep-ph]].
- [16] D. E. Kaplan, K. Rehermann, M. D. Schwartz and B. Tweedie, Phys. Rev. Lett. **101**, 142001 (2008) [arXiv:0806.0848 [hep-ph]]; S. Rappoccio [CMS Collaboration], PoS E **PS-HEP2009**, 360 (2009); T. Plehn, M. Spannowsky, M. Takeuchi and D. Zerwas, arXiv:1006.2833 [hep-ph].